Route diversity analyses for free-space optical wireless links within turbulent scenarios

Stanislav Zvanovec,[1,*] Joaquin Perez,[2] Zabih Ghassemlooy,[2] Sujan Rajbhandari,[3] and Jiri Libich[1]

[1]*Department of Electromagnetic Field, Czech Technical University in Prague, 2 Technicka, 16627 Prague, Czech Republic*

[2]*Optical Communications Research Group, Faculty of Engineering and Environment, Northumbria University, NE1 8ST, Newcastle Upon Tyne, UK*

[3] *Department of Engineering Science, University of Oxford, Parks Road OX1 3PJ, Oxford, UK*

[*]*xzvanove@fel.cvut.cz*

Abstract: Free-Space Optical (FSO) communications link performance is highly affected when propagating through the time-spatially variable turbulent environment. In order to improve signal reception, several mitigation techniques have been proposed and analytically investigated. This paper presents experimental results for the route diversity technique evaluations for a specific case when several diversity links intersects a common turbulent area and concurrently each passing regions with different turbulence flows.

OCIS codes: (060.2605) Free-space optical communication; (010.1330) Atmospheric turbulence; (060.4510) Optical communications.

References and links

1. Z. Ghassemlooy, W. Popoola, and S. Rajbhandari, *Optical Wireless Communications: System and Channel Modelling with MATLAB* (CRC, 2012).
2. M. Grabner and V. Kvicera, "The wavelength dependent model of extinction in fog and haze for free space optical communication," Opt. Express **19**(4), 3379–3386 (2011).
3. J. Perez, Z. Ghassemlooy, S. Rajbhandari, M. Ijaz, and H. Minh, "Ethernet FSO communications link performance study under a controlled fog environment," IEEE Commun. Lett. **16**(3), 408–410 (2012).
4. Z. Ghassemlooy, H. Le Minh, S. Rajbhandari, J. Perez, and M. Ijaz, "Performance analysis of ethernet/fast-ethernet free space optical communications in a controlled weak turbulence condition," J. Lightwave Technol. **30**(13), 2188–2194 (2012).
5. X. Zhu and J. M. Kahn, "Performance bounds for coded free-space optical communications through atmospheric turbulence channels," IEEE Trans. Commun. **51**(8), 1233–1239 (2003).
6. W. Gappmair, "Further results on the capacity of free-space optical channels in turbulent atmosphere," IET Commun. **5**(9), 1262–1267 (2011).
7. M. A. Khalighi, N. Schwartz, N. Aitamer, and S. Bourennane, "Fading reduction by aperture averaging and spatial diversity in optical wireless systems," J. Opt. Commun. Netw. **1**(6), 580–593 (2009).
8. T. A. Tsiftsis, H. G. Sandalidis, G. K. Karagiannidis, and M. Uysal, "Optical wireless links with spatial diversity over strong atmospheric turbulence channels," IEEE Trans. Wirel. Comm. **8**(2), 951–957 (2009).
9. S. M. Navidpour, M. Uysal, and M. Kavehrad, "BER performance of free-space optical transmission with spatial diversity," IEEE Trans. Wirel. Comm. **6**(8), 2813–2819 (2007).
10. H. Moradi, H. H. Refai, and P. G. LoPresti, "Switch-and-stay and switch-and-examine dual diversity for high-speed free-space optics links," IET Optoelectron **6**(1), 34–42 (2012).
11. R. K. Tyson, "Bit-error rate for free-space adaptive optics laser communications," J. Opt. Soc. Am. A **19**(4), 753–758 (2002).
12. V. Weerackody and A. R. Hammons, "Wavelength Correlation in Free Space Optical Communication Systems," in *Proceedings of IEEE Military Communications Conference 2006*, (IEEE, 2006), pp. 1–6.
13. J. A. Anguita, M. A. Neifeld, and B. V. Vasic, "Spatial correlation and irradiance statistics in a multiple-beam terrestrial free-space optical communication link," Appl. Opt. **46**(26), 6561–6571 (2007).
14. N. D. Chatzidiamantis, A. S. Lioumpas, G. K. Karagiannidis, and S. Arnon, "Adaptive subcarrier PSK intensity modulation in free space optical systems," IEEE Trans. Commun. **59**(5), 1368–1377 (2011).
15. S. Rosenberg and M. C. Teich, "Photocounting Array Receivers for Optical Communication through the Lognormal Atmospheric Channel. 2: Optimum and Suboptimum Receiver Performance for Binary Signaling," Appl. Opt. **12**(11), 2625–2635 (1973).

#183362 - $15.00 USD Received 11 Jan 2013; revised 18 Feb 2013; accepted 11 Mar 2013; published 20 Mar 2013

16. A. Belmonte, A. Comerón, J. A. Rubio, J. Bará, and E. Fernández, "Atmospheric-turbulence-induced power-fade statistics for a multiaperture optical receiver," Appl. Opt. **36**(33), 8632–8638 (1997).
17. M. Jeganathan, M. Toyoshima, K. Wilson, J. James, G. Xu, and J. Lesh, "Data analysis results from the GOLD experiments," Proc. SPIE **2990**, 70–81 (1997).
18. F. G. Walther, S. Michael, R. R. Parenti, and J. A. Taylor, "Air-to-Ground Lasercom System Demonstration Design Overview and Results Summary," Proc. SPIE **7814**, 78140Y, 78140Y-9 (2010).
19. E. J. Lee and V. W. S. Chan, "Part 1: Optical communication over the clear turbulent atmospheric channel using diversity," IEEE J. Sel. Areas Comm. **22**(9), 1896–1906 (2004).
20. N. Letzepis, K. D. Nguyen, A. G. Fabregas, and W. G. Cowley, "Outage analysis of the hybrid free-space optical and radio-frequency channel," IEEE J. Sel. Areas Comm. **27**(9), 1709–1719 (2009).
21. E. Lee, J. Park, D. Han, and G. Yoon, "Performance analysis of the asymmetric dual-hop relay transmission with mixed RF/FSO links," IEEE Photon. Technol. Lett. **23**(21), 1642–1644 (2011).
22. W. O. Popoola, Z. Ghassemlooy, H. Haas, E. Leitgeb, and V. Ahmadi, "Error performance of terrestrial free space optical links with subcarrier time diversity," IET Commun. **6**(5), 499–506 (2012).
23. W. O. Popoola, Z. Ghassemlooy, J. I. H. Allen, E. Leitgeb, and S. Gao, "Free-space optical communication employing subcarrier modulation and spatial diversity in atmospheric turbulence channel," IET Optoelectron **2**(1), 16–23 (2008).
24. COST action IC 1101 OPTICWISE Optical Wireless Communications - An Emerging Technology", retrieved 20.11.2012, *http://opticwise.uop.gr/*.
25. A. Kashyap, K. Lee, M. Kalantari, S. Khuller, and M. Shayman, "Integrated topology control and routing in wireless optical mesh networks," Comput. Netw. **51**(15), 4237–4251 (2007).
26. J. Libich, S. Zvanovec, and M. Mudroch, "Mitigation of time-spatial influence in free-space optical networks utilizing route diversity," Proc. SPIE **8246**, 82460O (2012).
27. S. Kaneko, T. Hamai, and K. Oba, "Evaluation of a free-space optical mesh network communication system in the Tokyo metropolitan area," J. Opt. Netw. **1**, 414–423 (2002).
28. W. K. Pratt, *Laser Communication Systems* (John Wiley & Sons, 1969).
29. S. Karp, R. M. Gagliardi, S. E. Moran, and L. B. Stotts, *Optical Channels: Fibers, Clouds, Water and the Atmosphere* (Plenum, 1988).
30. G. R. Osche, *Optical Detection Theory for Laser Applications* (Wiley-Interscience, 2002).
31. A. Kolmogorov, ed., *Turbulence*, Classic Papers on Statistical Theory (Wiley-Interscience, 1961).
32. L. C. Andrews and R. L. Phillips, *Laser Beam Propagation through Random Media* (SPIE, 2nd edition, 2005).
33. Y. C. Ko, M. S. Alouini, and M. K. Simon, "Analysis and optimization of switched diversity systems," IEEE Trans. Vehicular Technol. **49**(5), 1813–1831 (2000).

1. Introduction

Time-variant influence of the atmosphere in FSO links introduces one of the main drawbacks when used in place of slower (in terms of data rate) microwave links or in situations where there are no available fiber optical links [1]. Fog is the biggest problem in FSO systems and has been studied extensively in the literature [2, 3]. The atmospheric thermal induced turbulence is the next factor that has the high impact on the FSO link performance by affecting the statistics of the received signal [4]. The scintillations caused by variation in the reflective index due to the temperature and pressure fluctuations result in random variations of light intensities in both space and time at the receiver plane. In the clear weather conditions, theoretical and experimental studies have shown that scintillation could severely affect the FSO link reliability and availability at all times [5, 6]. Scintillation has been investigated extensively and a number of theoretical models have been proposed to describe the scintillation induced fading [4, 6–8].

In order to overcome the turbulence induced fading in FSO systems, several techniques have been proposed. These include: spatial transmitter/receiver diversity [9] [10]; adaptive beam forming based on the wave front phase error measurement and settings of the opposite phase aberration on the beam by a deformable mirror [11]; wavelength diversity [12], multiple-beam communication [13] and novel modulation techniques [14]. SIMO (single-input multiple-output) or MIMO (multiple-input multiple-output) optical channels have been studied for more than 40 years [15, 16] and measurements of SIMO systems were reported in numerous papers, e.g. between terrestrial station and satellite [17], ground station and aircraft [18] or laboratory experiments [13, 19]. Approximations to the probability density function of the received power of a partially spatially correlated multiple-beam system have been proposed in relation to the single-channel gamma–gamma link function. But to authors' best

#183362 - $15.00 USD Received 11 Jan 2013; revised 18 Feb 2013; accepted 11 Mar 2013; published 20 Mar 2013

knowledge no joint statistics of turbulence enumerated from the measured thermal distribution of an FSO link together with received optical signal fluctuations have been reported yet. A hybrid RF/optical link scheme [20, 21] offers 100% link availability and improved outage probability statistics, but at the cost of additional switching and buffering when using the RF link at a very high data rate, thus limiting the available data rates.

The error performance and the outage probability of a subcarrier intensity modulation (SIM) system employing the spatial and temporal diversity schemes to combat the channel fading in the optical region were discussed in [22]. SIM with phase shift keying (PSK) has been considered as an alternative for the turbulence induced fading mitigation and can be applied in combination with the spatial diversity [23]. In [23] the log-normal, gamma-gamma and negative exponential atmospheric turbulence models have been extensively investigated and the error performance in case of SIMO FSO links have been derived for three different linear combining techniques – Maximal Ratio Combining (MRC), Equal Gain Combining (EGC) and Selection Combining (SelC). It was illustrated that both multiple transmitter-single photodetector and single transmitter-multiple photodetector configurations employing EGC offer the same performance in a turbulence condition. The number of independent photodetectors capable of mitigating the scintillation without overwhelming complexity is reported to be approximately between two and four [23]. The subcarrier time delay diversity (TDD) was presented as an alternative technique for ameliorating the channel fading and its error performance was analyzed in [22]. Retransmitting the delayed copy of the information just once was found to be the optimum with a gain of up to 4.5 dB in the weak atmospheric turbulence condition. The TDD gain was shown to be proportional to the fading strength but independent of the data rate.

The above mentioned cases introduced mostly analytically and statistically based models. It is worth mentioning that the experimental verifications including both continuous measurements of time-space changes in the atmosphere together with statistics of wireless optical links have been reported very scarcely and there is a lack of measurement data from wide range of measurement sites. Therefore, as part of the European COST (Cooperation in Science and Technology) action IC 1101 – OPTICWISE (Optical Wireless Communications – An Emerging Technology) [24] is to put together a common database of measuring sites, measured data and available software codes etc. with the aim of better understanding problems and developing theoretical and empirical models.

To fully comprehend the turbulence phenomena for complex FSO networks, the original analysis of the influence of turbulence on the simple fragment of such a network with two route diversity links (from either two different distant points to the joint network node or in the reverse direction) had to be accomplished. In [25] the focus had been on the understanding of the route diversity concept from the point of view of the turbulence scenarios and how it affected the performance of the FSO networks. From the measurement performed in the university campus of the Czech Technical University in Prague, it was determined that the diversity gain of the joint three optical wireless links can yield from 2 dB to 9 dB for 99.9% and 99.9999% availability, respectively when tested using a multi FSO/RF network [26]. In [27] another route diversity application for the mesh optical networks was introduced together with interesting experiment results.

The main aim of this paper is to report original experimental results determining the specific case when links are experiencing two distinctive turbulence conditions: (i) partially correlated turbulence channels, and concurrently (ii) non-correlated turbulence channels only for part of selected diversity link.

2. Measurement setup

The indoor laboratory atmospheric chamber has been developed to enable quick performance assessment of the FSO link under a controlled environment [4]. This indoor chamber offers the advantage of full FSO systems characterization and investigation in much less time

#183362 - $15.00 USD Received 11 Jan 2013; revised 18 Feb 2013; accepted 11 Mar 2013; published 20 Mar 2013

compared to outdoor FSO, where it could take a long time for the weather conditions to maintain a regular behavior and changes that could not be accurately predicted therefore prolonging the characterization and measurements.

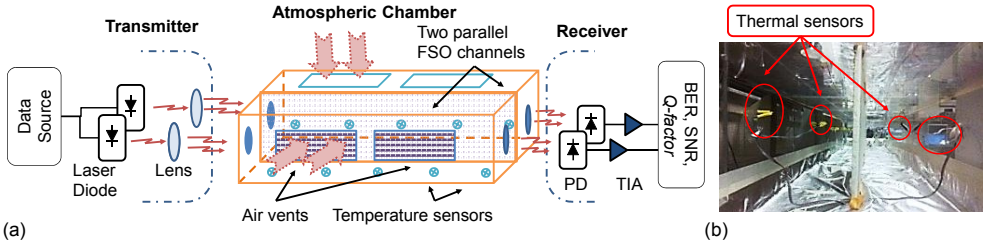

Fig. 1. (a) Block diagram of the laboratory turbulence chamber; (b) snapshot of the deployment of thermal sensor line inside the chamber.

Table 1. Parameters of the optical wireless Link

Transmitter parameters		
Data source	Line-rate R_b	1 Mbit/s
	Format	NRZ
Laser diode modules	Peak wavelength	830 nm / 670 nm
	Maximum optical power	10 mW / 10 mW
	Class	3B
	Beam size at aperture	5 mm × 2 mm
	Beam divergence	5 mrad
	Laser beam propagation model	Plane
	Modulation bandwidth	50 MHz
Receiver parameters		
Photoreceiver	Type	Si PIN
	Spectral range of sensitivity	200-1100 nm
	Active area	0.8 mm^2
	Spectral sensitivity	0.38 A/W at 830 nm 0.39 A/W at 670 nm
	RF bandwidth	150 MHz

The experimental measurement set-up using the laboratory atmospheric chamber is depicted in Fig. 1(a). At the transmitter side two narrow divergence beam laser sources plus a collimated lens are used. The optical beams are modulated by a data source at a line-rate of 1 Mbit/s. The laboratory atmospheric channel is a closed glass chamber with a dimension of 5.5 × 0.3 × 0.3 m. The chamber has air vents with external fans for air circulation along its length to control the temperature distribution. External heaters are used to pump hot air into the chamber to create the turbulence. The room temperature is around 20 - 25 °C, this range is considered as the cold or the baseline temperature reaching up to 60 °C. There are also 19 remotely controlled thermal sensors positioned along the chamber monitoring and taking measurement of the temperature at every one second interval within a range of −55 °C to + 125°C and a resolution of 0.1 °C, see Fig. 1(b). The receiver front-end consists of a PIN photodetector and a transimpedance amplifier (TIA). The TIA output signal is captured using a wide bandwidth real time digital oscilloscope and a full signal analysis is carried out off line in Matlab. The main parameters of the experimental system are given in Table 1.

The random fluctuation in the atmospheric temperature along the optical beam propagation path results in variation of the atmospheric refractive index n_{as} [28]. The rate of change of the atmospheric refractive index n_{as} depends on the atmosphere temperature and pressure as given by [29]:

#183362 - $15.00 USD Received 11 Jan 2013; revised 18 Feb 2013; accepted 11 Mar 2013; published 20 Mar 2013

$$n_{as} = 1 + 77.6\left(1 + 7.52\times10^{-3}\lambda^{-2}\right)\frac{P_{as}}{T_e}\times10^{-6}, \tag{1}$$

$$-dn_{as}/dT_e = 7.8\times10^{-5}P_{as}/T_e^2, \tag{2}$$

where P_{as} is the atmospheric pressure in millibars, T_e is the effective temperature in Kelvin and λ is the wavelength in micrometers. Near the sea level, $-dn_{as}/dT_e \cong 10^{-6}\,\mathrm{K}^{-1}$ [29]. The contribution of humidity to the refractive index fluctuation is not accounted for Eq. (1) because this is negligible at optical wavelengths [30].

In atmospheric turbulence, an important parameter for characterizing the amount of refractive index fluctuation is the index of the refraction structure parameter C_n^2 introduced by Kolmogorov [31], which is a function of the wavelength, pressure and temperature as given by [32]:

$$C_n^2 = \left(86\times10^{-6}\frac{P_{as}}{T_e}\right)^2 C_T^2, \text{at } \lambda = 850\text{nm}, \tag{3}$$

where the temperature structure constant C_T^2 is related to the universal 2/3 power law of temperature variation as given in:

$$D_T = \left\langle \left(T_1 - T_2\right)^2 \right\rangle = \begin{cases} C_T^2 l_0^{-4/3} L_p^2 & \text{for } 0 < L_p < l_0 \\ C_T^2 L_p^{2/3} & \text{for } l_0 < L_p < L_0 \end{cases}, \tag{4}$$

where T_1 and T_2 are the temperatures at two points separated by the propagation distance L_p, l_0 and L_0 stand for inner and outer scale of turbulence. Values of C_n^2 can vary from 10^{-17} $\mathrm{m}^{-2/3}$ up to 10^{-12} $\mathrm{m}^{-2/3}$ for weak and strong turbulence regimes, respectively. Due to their random nature, the turbulent media is extremely difficult to describe mathematically due to the presence of non-linear mixing of observable quantities [30]. A number of statistical models to describe optical intensity variation under various turbulence strengths had been proposed and studied. The two most popular among them is log-normal and Gamma-Gamma models.

The extent of field amplitude fluctuation in the atmospheric turbulence can be characterized by the log-amplitude variance σ_x^2, commonly referred to as Rytov parameter. σ_x^2 for a plane wave is related to C_n^2, the horizontal distance L_p travelled by the optical field/radiation as:

$$\sigma_x^2 = 0.56k^{7/6}\int_0^{L_p} C_n^2(x)\left(L_p - x\right)^{5/6} dx, \tag{5}$$

where $k = (2\pi/\lambda)$ is the spatial wave number. For a field propagating horizontally through the turbulent medium, as is the case in most terrestrial applications, the refractive index structure parameter C_n^2, is constant, and the log irradiance variance (scintillation index) for a plane wave becomes:

$$\sigma_i^2 = 1.23C_n^2k^{7/6}L_p^{11/6}, \tag{6}$$

where the log-intensity variance $\sigma_i^2 = 4\sigma_x^2$.

3. Experimental evaluation

3.1 Separated channels

A number of techniques have been proposed in the literature to deal with the turbulence including the aperture averaging, the spatial diversity, and the cooperative diversity, as

#183362 - $15.00 USD Received 11 Jan 2013; revised 18 Feb 2013; accepted 11 Mar 2013; published 20 Mar 2013

mentioned in the introduction section. As a first analysis, in this paper a pilot testing measurement was performed with multiple transmitters. Within the measured scenario the laser beam at 830 nm was split into two with each beam propagating through two 1 m long non-turbulent and turbulent channels and then through a 1 m long common channel, see Fig. 2(a). The reduced scintillation effect observed is mainly due to a small part of the propagation path being affected by different turbulences conditions. The diversity scheme was evaluated via a diversity gain, which is defined as the difference between attenuation of a single link and the minimum attenuation of joint diversity links. The diversity gain of the co-propagating beams received by the receivers separated by 0.08 m did not exceed 0.4 dB even in case of the turbulence condition with $C_n^2 > 10^{-11}$ m$^{-2/3}$. Therefore for the small scale turbulence phenomena it would be more beneficial to employ the aperture averaging scheme.

To validate statistical results, the channel separation was increased and measurements were carried out for two separate channels isolated by a divider and foils. The measurement set-up within the turbulence chamber is shown in Fig. 2(b). Channel 2 was influenced by a constant distortion or the impairment due to the intensity variation of the received signal, i.e. with Rytov variance being kept below 0.09. This small intensity variation is not considered to be due to the turbulence and is more to do with the material used to isolate both channels. In this case the foil is a transparent film sheet made of polyethylene terephthalate or polyester. The physical vibration of the foil is not significant to the human eye but does modify the intensity of the received signal, thus implying a small measured value of Rytov variance in the channel under study, however this small deviation and variance is not associated with the temperature effects. On the other hand, the turbulence in the channel 1 was gradually changed from low to moderate conditions.

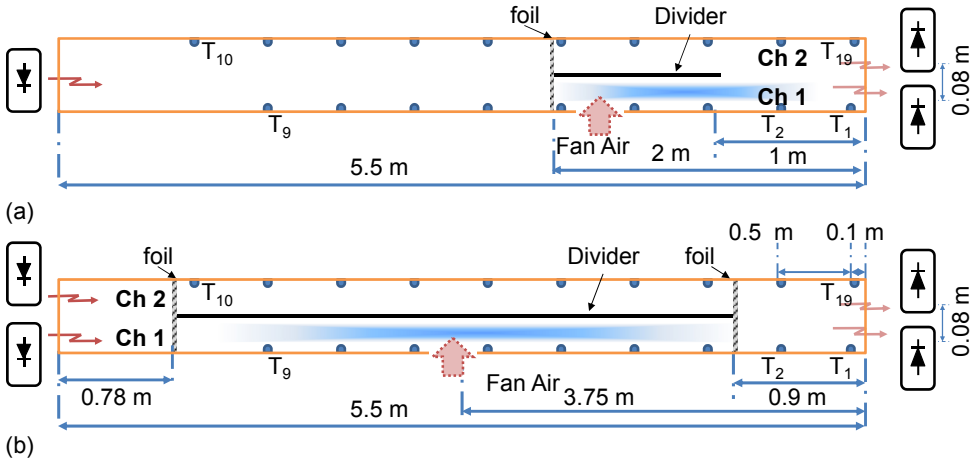

Fig. 2. Deployment for measurement of two separated channels, (a) unique laser source SIMO and (b) dual laser source for isolated channels configuration.

In Fig. 3(a) Rytov variance derived either from the fluctuation of received optical signal (enumerated with the correction of the effective area of the photodetector aperture averaging $\sigma_1^2(0)/\sigma_1^2(D) = 0.69$ in accordance to [7]) and from the thermal sensors derived by integration over the thermal distribution using Eq. (5) for the same parameters are presented. Red circles show particular measurements for channel 1 with increased turbulence levels while the blue crosses represent parallel measurements for channel 2. Even though initially there was no turbulence in channel 2, we experienced some deviations in channel 2 due to the flow around foils and its small vibration. As it can be seen, the variance in optical signal increases even though there is no linear dependence with thermal variations within the channel.

#183362 - $15.00 USD Received 11 Jan 2013; revised 18 Feb 2013; accepted 11 Mar 2013; published 20 Mar 2013

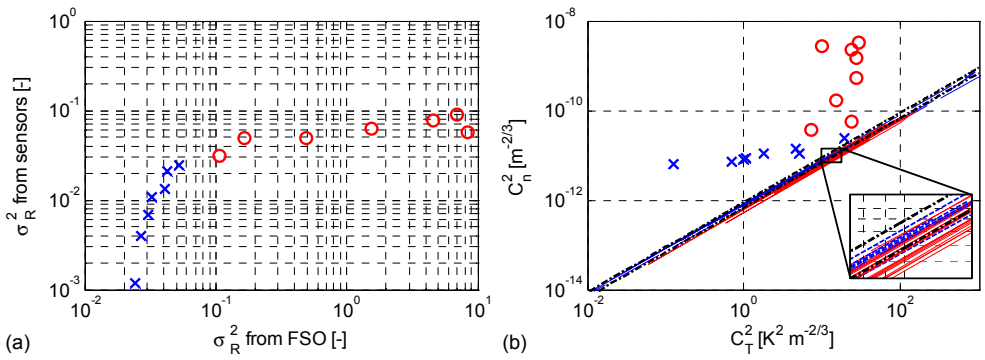

Fig. 3. Measured dependence of (a) Rytov variances in both channels derived from received optical signal and from thermal sensors measurements (symbols, red circles - channel 1, blue crosses - channel 2) and (b) C_n^2 theoretical relations (black dotted lines), C_n^2 derived from measured thermal distributions via Eqs. (3) and (4) (channel 1 red and channel 2 blue lines) and C_n^2 derived from measured of optical power on C_T^2 measured by the sensor line (symbols; red circles - channel 1, blue crosses – channel 2)

Figure 3(b) gives an insight to the ratio of the thermal structure and the refractive index structural parameters. Black dotted lines show theoretical C_n^2 dependence derived from Eq. (3) in case of the mean temperatures T_e 20°C and 40°C. Colored lines, see inset, represent C_n^2 values enumerated from each sensor gap for all turbulence sets according to Eqs. (3) and (4), i.e. based on measured thermal differences and ensemble averaged values (channel 1 depicted in red solid line, channel 2 in blue dashed line) and C_T^2. Finally, single points, red circles and blue crosses for channels 1 and 2, respectively, show the relations between two measured approaches - C_T^2 measured in channels via thermal distributions and C_n^2 observed through fluctuations of the received optical signal in terms of Rytov variance. C_n^2 values from three points of view are therefore compared: theoretical assumption, derivation from temperature fluctuations and enumeration of optical received fluctuations.

As can be seen, C_n^2 derived from thermal variation in turbulence conditions for particular sensor positions fully meets theoretical assumptions (colored and black lines, respectively). For the distributions of C_n^2, derived from Rytov variance, it is then evident that theoretical assumptions underestimate C_n^2 -to- C_T^2 ratio, which can be attributed principally to the integration over the link length to obtain C_T^2.

3.2. Partial correlation in turbulences at channels

When considering deployment of wireless networks in urban areas the route diversity technique may be adopted in order to ensure higher link availability. To combat link failures FSO links can be arranged in several possible topologies thus offering diversity within the network to ensure link availability at all times.

The main aim during laboratory experiments was to analyze the route diversity for two links for case of intersecting the same turbulence area (i.e. channel 2 and part of channel 1) with the fraction of linearly increasing turbulence zone covering the major part of channel 1. This scenario corresponds to the real case when two links within the network are terminating at the same point, i.e. passing the common volume with the same or almost similar turbulence characteristic. Note one of the optical links is along the distant part influenced by the non-correlated turbulent flow. The measurement deployment can be seen in Fig. 4.

#183362 - $15.00 USD Received 11 Jan 2013; revised 18 Feb 2013; accepted 11 Mar 2013; published 20 Mar 2013

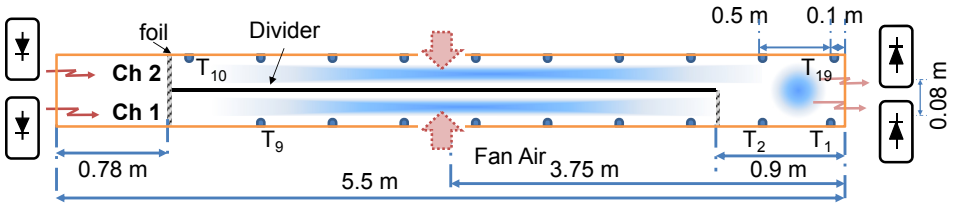

Fig. 4. Deployment for measurement of partially correlated turbulences within channels

Contrary to the previous case, the turbulence level in channel 2 was kept at Rytov variance value of ~0.07. Compare the dependency of C_n^2 on C_T^2 (Fig. 5), we observed that there is a decrease in the slope for the moderate turbulence condition, see inset in Fig. 5.

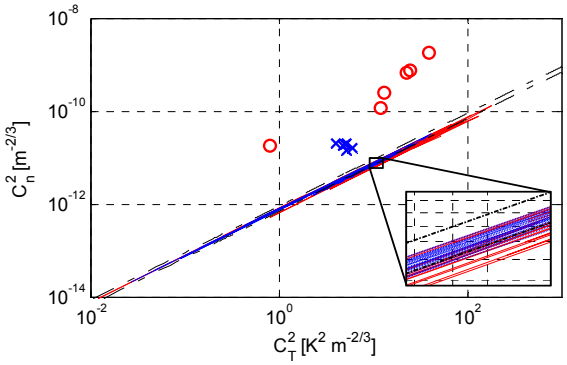

Fig. 5. Dependence of C_n^2 derived from measured of optical power measurements (red circles – channel1, blue crosses - channel 2) and from sensor line on thermal structural parameter in case of partially correlated turbulences, temperature measurements from channel 1 (red solid lines) and channel 2 (blue dashed lines) line sensors, compared with C_n^2 dependence derived from Eqs. (3) and (4) for the mean temperatures of 20°C and 40°C (black dotted lines)

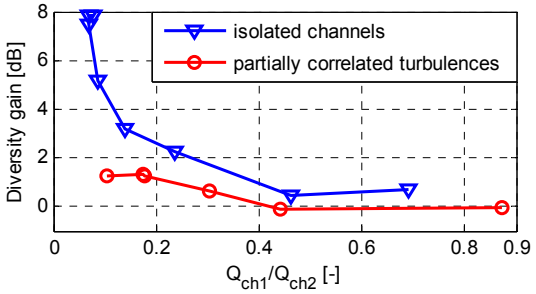

Fig. 6. Comparison of diversity gains for two different turbulence scenarios with respect to Q-factor ratio between channels

In the next step, the diversity gains were derived in relation to *Q*-factors of received OOK signal from offline signal processing of both channels. The diversity gain against the *Q*-factor ratio between the channel with a low turbulence level and channels with high turbulence levels expressed by Q_{ch1}/Q_{ch2} is shown in Fig. 6. This *Q*-factor ratio expresses the relation of behavior between both channels. Regarding Fig. 6, for the case of two isolated channels, there is an obvious enhancement in the received power when under particular signal fade the receiver is able to switch to the second (less affected) channel. This corresponds to similar characteristics derived analytically for the SelC diversity method [23]. To reduce the high processing load (thus the complexity) in SelC switched combining diversity, the switch-and-stay combining (SSC) and switch-and-examine combining (SEC) diversity schemes are

#183362 - $15.00 USD Received 11 Jan 2013; revised 18 Feb 2013; accepted 11 Mar 2013; published 20 Mar 2013

introduced. In SSC, once the existing received SNR drops below a certain threshold level, the combiner switches to the next branch, regardless of SNR for the new branch even if it is less than the original branch. In SSC and SEC diversity schemes there is no need for continual monitoring of all receiving signals, thus leading to a much simplified receiver design compared to SelC at the cost of inferior performance [10, 33].

The SelC linear combiner samples the entire received signal through multiple branches and selects the branch with the highest SNR value or the irradiance level, provided the photodetectors receive the same amount of background radiation. The output is equal to the signal on only one of the branches and not the coherent sum of the individual photocurrents as is the case in MRC and EGC. This makes SelC suitable for differentially modulated, non-coherent demodulated subcarrier signals. In addition, SelC is of reduced complexity compared to the MRC and EGC and its conditional SNR is given by:

$$\gamma_{SelC}(I) = \frac{R^2 A^2 I_{\max}^2}{2N\sigma^2}, \tag{7}$$

where $I_{max} = \max(I_1, I_2, \ldots, I_N)$. The pdf of the received irradiance, $p(I_{\max})$, given by Eq. (8), is obtained by first determining its cumulative density function (cdf) and then differentiating.

$$p(I_{\max}) = \frac{2^{1-N} N \exp\left(-y^2\right)}{I\sigma_i\sqrt{2\pi}}\left[1+\operatorname{erf}(y)\right]^{N-1}, \tag{8}$$

where

$$y = \frac{\ln\left(I/I_0\right) + \sigma_l^2/2}{\sqrt{2}\sigma_l}. \tag{9}$$

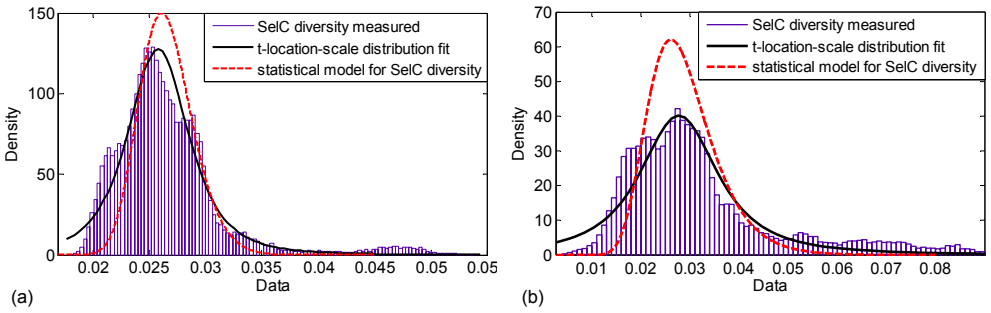

Fig. 7. Examples from comparisons of measured and calculated Selection Combining diversity with Rytov variance in channels (a) $\sigma_1^2 = 0.0305$, $\sigma_2^2 = 1.5606$, (b) $\sigma_1^2 = 0.0608$, $\sigma_2^2 = 5.4235$

From the measurements it was observed that the above mentioned analytical assumptions lead to overestimation of received signal deviation in case of two channels crossing non-correlated turbulences. As can be seen in Fig. 7 from comparison of probability density functions of the measured route diversity data and the statistically derived pdf by Eq. (8) there is higher deviation in the measured selection diversity signal than expected. With increased turbulence levels in one of the channels we experienced heavier tails of pdf. Even though Eq. (8) in majority cases introduces quite a precise estimate it was derived that the combined diversity statistics of the received route diversity signal follow the modified Student's t-distribution with N-degree of freedom (corresponding to number of channels, i.e. in our case $N = 2$) described by the density function:

#183362 - $15.00 USD Received 11 Jan 2013; revised 18 Feb 2013; accepted 11 Mar 2013; published 20 Mar 2013

$$p = \frac{\Gamma\left(\frac{N+1}{2}\right)}{\sigma\sqrt{N\pi}\,\Gamma\left(\frac{N}{20}\right)}\left[\frac{N+\left(\frac{I-I_0}{0.1\sigma}\right)^2}{N}\right] \tag{10}$$

Results from the second measurement set-up (see Fig. 4) indicates that the increment in transmitted optical power or switching to the second diversity link will have a reduced effect under the increased turbulence levels when both channels intersect a common turbulence area (red curve in Fig. 6). Comparison of the diversity gains with respect to the mean C_n^2 ratio between both the channels is given in Fig. 8. With increased turbulence level from low towards moderate in channel 2, the system is more efficient with the route diversity scheme when both channels experience different turbulences along their links compare to the case when both links pass through a common turbulent channel.

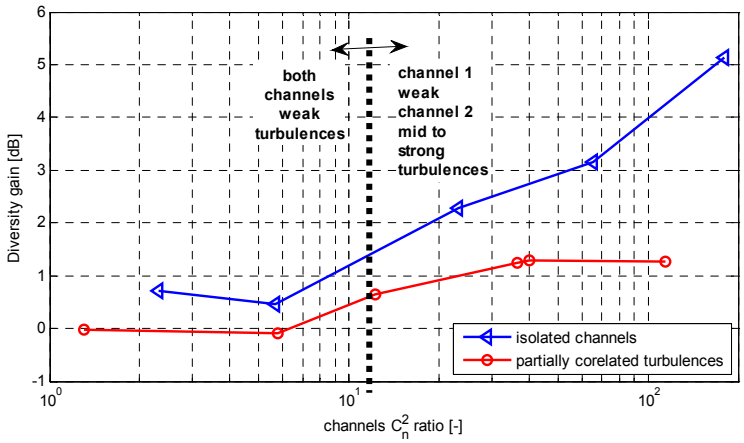

Fig. 8. Comparison of diversity gains for two different turbulence scenarios with respect to C_n^2 ratio between channels

5. Conclusion

The route diversity techniques for an FSO link were evaluated based on the experimental work for a specific case where a number of diversity links is investigated for both a common turbulent channel and a channel with different turbulence regimes. When compared to the isolated link channels the total optical signal deviations follows different probability density, which is more appropriately described by the t-location-scale distribution. Contrary to non-correlated turbulence channels, the utilization of route diversity do not contributed significantly to the enhancement of the received optical signal in case of correlated turbulence. This phenomenon is more distinguishable with the increased level of turbulence strength. Based on the original measurement results more complex system analyses will be performed in next research steps.

Acknowledgments

This research project forms part of the both teams activities within the frame of COST ICT Action IC1101 - Optical Wireless Communications - An Emerging Technology (OPTICWISE). Publication was supported by the MEYS CR grant LD12058.